Chemistry Africa (2019) 2:673–688
https://doi.org/10.1007/s42250-019-00072-z

ORIGINAL ARTICLE

Amberlite XAD-2010 Impregnated with Chrome Azurol S for Separation and Spectrophotometric Determination of Uranium and Thorium

Ahmed Hussien Orabi[1] · **S. A. Elenein**[2] · **Sh. S. Abdulmoteleb**[1]

Received: 2 March 2019 / Accepted: 28 May 2019 / Published online: 1 June 2019

Abstract

A new extractant-impregnated resin (EIR), chrome azurol S-impregnated on XAD-2010, is used as an adsorbent to separate and preconcentrate U(VI) and Th(IV) ions prior to their spectrophotometric determination. Various instrumental techniques such as elemental analysis, FTIR, and SEM analysis were employed for full characterization of the synthetic extractant. Optimization of the adsorption and elution conditions of U(VI) and Th(IV) ions using synthesized chrome azurol S-impregnated XAD-2010 were studied. Langmuir isotherm model has the best fitting experimental data with a maximum adsorption capacity of 23.8 mg g^{-1} for U(VI) and 25.4 mg g^{-1} for Th(IV). The adsorption process of each metal ion using synthesized chrome azurol S-impregnated XAD-2010 showed an exothermic pseudo-second-order adsorption process. High tolerance limits for several studied metal ions on chrome azurol S-impregnated XAD-2010 were observed. The optimized method was applied on an international certified samples and different rock types bearing thorium and uranium with accurate results.

Keywords Separation · Spectrophotometric · Uranium · Thorium · Chrome Azurol S-impregnated XAD-2010 · Rocks

1 Introduction

The strategic issue of chemists is the exploration and mining besides the processing of the ore materials containing nuclear elements such as uranium and thorium, which represents the corner stone of the (industrial) nuclear technology [1, 2].

Furthermore, their accurate determination using several advanced and simple techniques with economic procedures was of great prominence for precise and accurate evaluation of their occurrences in certain areas [3–5].

Problems encountering the spectrophotometric technique (as a simple cheap and available technique) are mainly referring to spectral interference. In this situation, matrix constituents of rock can be considered as the ordinary factor disturbing elemental measurements. The spectral interference enhances the uranium and thorium absorbance value giving incorrect concentration values [6, 7].

To solve this problem, the segregation including coprecipitation, solvent extraction, electrodeposition, ion-exchange etc. [8–14] has been used in the analytical chemistry laboratories for their precise and accurate determination. Solid phase extraction (SPE) is one of the efficient preconcentration-differentiation procedures used, due to its simplicity and confined usage of the organic solvents [15–24]. Solid phase extraction of thorium and uranium is also a preferable choice in analytical chemistry in common [25–33].

The Amberlite XAD resins are extremely important from both the economic and environmental point of views for solid phase extraction after their proper functionalization [34–36]. The literature survey revealed that XAD-2000 and XAD-2010 are used for the preconcentration and seclusion of organic materials at trace levels [37, 38]; however, only few studies on these resins were highlighted for preconcentration of trace metals [39–41].

To achieve accurate and precise determination of both elements, spectrophotometric method using the proper sensitive and selective dye was merged with solid phase extraction technique in this work. In the pursuance of many researches on the extractant impregnated resins

---

✉ Ahmed Hussien Orabi
A_orabi_chem@yahoo.com

[1] Nuclear Materials Authority, Maadi, PO Box 530, Cairo, Egypt

[2] Chemistry Department, Faculty of Science, Menofia University, Shibin El Kom, Egypt

(EIRs) applications [27, 28, 42–47], this work converges on the eclectic separation and preconcentration of trace amounts of thorium and uranium in their bearing rocks using a new EIR containing Amberlite XAD-2010 resin beads impregnated with chrome azurol S. The new EIR adsorbent manifested eminent selectivity for thorium and uranium sorption from aqueous solutions after adequate optimization.

2 Experimental

2.1 Reagents

Chrome azurol S (CAS) and Amberlite XAD-2010 were purchased from Sigma Chemicals.

All the common reagents were supplied by VWR BDH Prolabo Chemicals (Fontenay-sous-Bois, France). On the other hand, U(VI), Th(V), Na(I), K(I), Ca(II), Mg(II), Al(III), Mn(II), Fe(III), Cr(VI), VO(II), Cu(II), Co(III), Ln(III), pb(II), Ba(II), Mo(VI), B(III), Cd(II), and Zn(II) standard stock solutions, 1000 ppm, were analytical grade and purchased from Merck (Darmstadt, Germany).

2.2 Preparation of the EIR

The CAS-impregnated XAD-2010 resin beads were prepared using a dry procedure [43]. Before the impregnation process, a pretreatment of Amberlite XAD-2010 resin beads were handled with 1:1 methanol–water solution comprising 6 M HCl for 12 h in order to drive out any enduring monomers and other species of impurities which may be found with the fabricated beads. The resin was totally rinsed with double-distilled water and placed into a drying oven at 323°K for 30 min. To prepare the impregnated resin, portions of Amberlite XAD-2010 resin (1 g of dry resin) were carried into a spectrum of glass stoppered bottles containing different concentrations of CAS in 200 mL methanol, which was utilized as a solvent. The entire contents were slowly shaken for 10 h to accomplish impregnation process and then heated at 333°K in a drying oven to drive out the solvent. Each EIR sample was then conveyed to a porous filter and washed consecutively with HCl (3 M) solution and enormous amounts of distilled water until no color of CAS dye was found in the filtrate. Eventually, the impregnated resins were dried at 323°K and weighed. Compound structure was characterized by means of SEM using a Jeol (Tokyo, Japan) JSM 5600 LV scanning electron microscope, FTIR spectrometer Bruker Vector 22 Germany in the range of 400–4000 cm^{-1}, and elemental analysis.

2.3 Analytical procedures

U and Th were spectrophotometerically determined by using the chromogenic reagents, Arsenazo-III and thoron I, respectively [48]. Other interfering elements were analyzed using Inductively Coupled Plasma Optical Emission Spectrometer (ICP-OES), Teledyne technologies.

2.4 Statistical and accuracy evaluation

Statistical techniques are applied, in the present work, in two ways: one of them is for estimating precision and accuracy of the analytical data and the second is for quality assurance of the produced concentrate. A common practice in analytical chemistry literature is to quote the mean ($\overline{X}$) as a common factor for estimating the precession (degree of reproducibility or random error). Accuracy (Δ) of a measurement method is defined as the measure of the closeness of results to reference (well known) or true one. The following equations are therefore applied [49–51]:

$$\text{Arithmetic mean: -}\quad \overline{X} = \frac{\sum X_i}{n}, \tag{1}$$

where Xi = is an individual measurement, n = is the number of measurements:

$$\text{Standard deviation: -}\quad SD = \left[\frac{\sum_1^n (X_i - \overline{X})^2}{(n-1)}\right]^{1/2}, \tag{2}$$

$$\text{Relative standard deviation: -}\quad RSD = SD\big/\bar{X} \times 100, \tag{3}$$

$$\text{Standard error: -}\quad SE = \frac{SD}{\sqrt{n}}, \tag{4}$$

$$\text{The percentage error: -}\quad \%\text{Error} = SE\big/\bar{X} \times 100, \tag{5}$$

$$\text{Accuracy: -}\quad \Delta = \pm\sqrt{\frac{d^2}{2n}}, \tag{6}$$

where d represents the difference between the repeated measurements.

2.5 Adsorption procedure

The adsorption process used batch technique to study different parameters affecting uranium and thorium adsorption process for the prepared EIR in all experiments such as pH, contact time, initial metal concentration, temperature and interfering ions. Thus, a sample (S) weight of 0.1 g (m) was added to a volume of 50 Ml (*V*) of U or Th aqueous solutions and equilibrated by stirring at room temperature. After a certain time, the solutions were filtered and the concentration of uranium and thorium was spectrophotometrically determined. Both the determination of the adsorption coefficient (Ads %) and the adsorption capacity (q) was calculated using the following equations:

$$q = \left(\frac{(C_i - C_f)}{m}\right) \times V, \tag{7}$$

$$Ads\% = \left(\frac{(C_i - C_f)}{Ci}\right) \times 100, \tag{8}$$

where, C_i and C_f are the initial and the final concentrations of aqueous phases, respectively.

3 Results and Discussion

3.1 Preparation of CAS-Impregnated Resin

Chrome azurol S dye (CAS) contains hydroxyl, carbonyl and sulphonate groups which make it suitable for chelating with several metal ions. Chrome azurol S -impregnated XAD-2010, CAS/XAD-2010, was efficiently prepared by the impregnation method, described in the experimental section. To prepare the suitable form of CAS/XAD-2010, various impregnation ratios; g CAS g^{-1} dry XAD-2010 adsorbent were studied and the data was illustrated in Fig. 1. As shown, the weight change increases as the impregnation ratio increases after which a plateau is reached at the impregnation ratio of 1.5 g CAS g^{-1} dry XAD-2010 adsorbent, where it was adopted as the optimum impregnation ratio.

3.2 Characterization of the Modified Resin

In order to verify the presence of the active functional groups of CAS in the modified resin, IR spectra of Amberlite XAD-2010 and the CAS/XAD-2010 modified resin were studied (Fig. 2). The IR spectrum of Amberlite XAD 2010 resin exhibited less intense band at 3436 cm^{-1}, which can be attributed to the stretching vibrations of adsorbed water [52]. The bands at 2924 cm^{-1} and 1632 cm^{-1} are assigned to the aliphatic—CH_2–CH_2 chains and the phenyl rings, respectively. The frequency at 1482 cm^{-1} is assigned to C=C stretching mode, while the peaks from 829 to 1120 cm^{-1} are attributed to C–C stretching vibrations. Upon modification with CAS, the phenolic-OH band appears at 3432 cm^{-1}. The most noticeable change in the spectra is the band at 1274 and 1213 cm^{-1} which are due to the stretching SO_3^{2-} band, while C–Cl band appeared at 572 cm^{-1}. Moreover, the bands were assigned to C–O at 1121–1033 cm^{-1} and the C=O band at 1625 cm^{-1}. The above mentioned bands indicate the modification of Amberlite XAD 2010 with CAS.

The CHNS elemental analysis of Amberlite XAD-2010 and the CAS/XAD-2010 modified resin were studied (Table 1). The elemental analysis of the CAS/XAD-2010 was conducted with an erratic increase in the C, H and N contents than Amberlite XAD-2010. In addition, the presence of S element (1%) confirms the impregnation of CAS into Amberlite XAD-2010 as shown in Table 1.

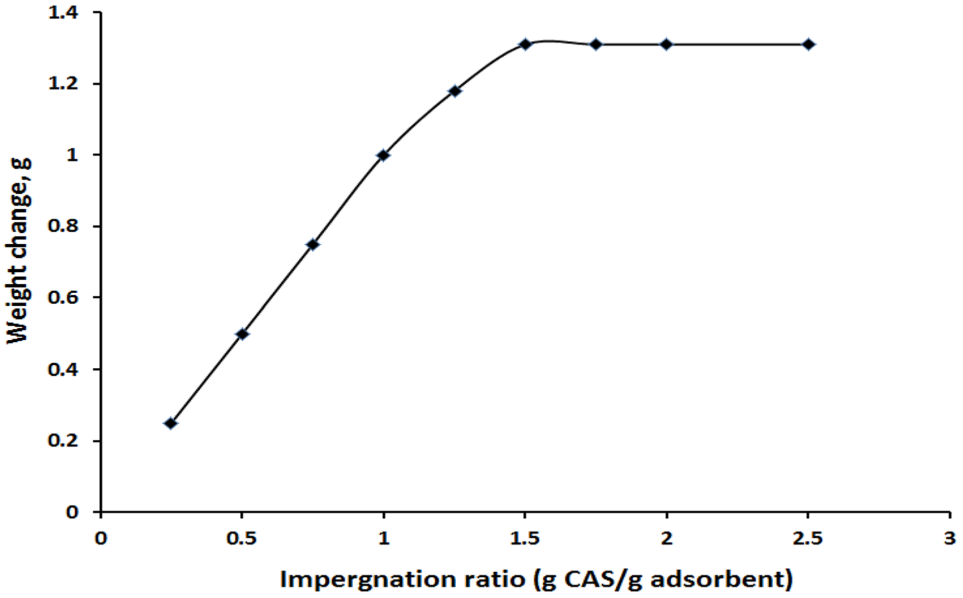

Fig. 1 Effect of the impregnation ratio on the EIR preparation at the condition that portions of 1-g of the dry polymer beads of Amberlite XAD-2010 was subjected to the impregnation process

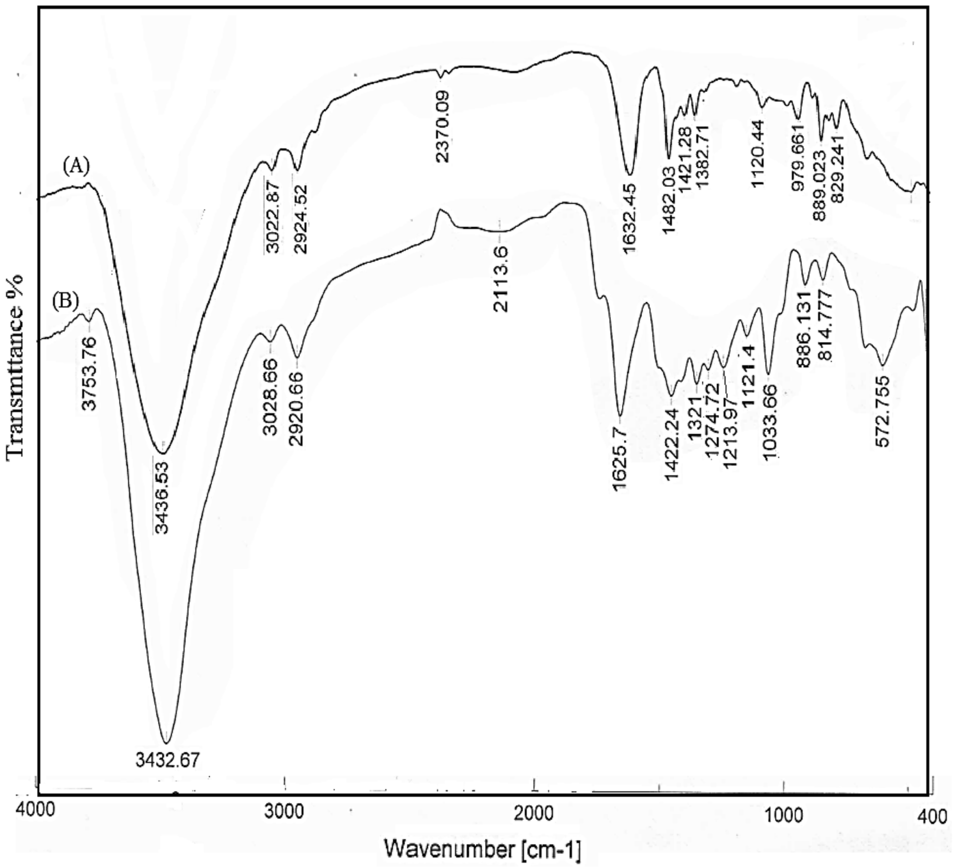

Fig. 2 FTIR spectroscopy of the working polymeric resin: **a** Amberlite XAD-2010 and **b** CAS/XAD-2010 modified resin

Table 1 The CHNS elemental analysis (weight %) of Amberlite XAD-2010 and the CAS/XAD-2010 modified resin

Sample	C	H	N	S
Amberlite XAD-2010	75.77	6.30	3.63	–
CAS/XAD-2010 modified resin	83.36	7.93	4.34	1.00

3.3 Effect of Acid Medium

From the critical parameters for solid phase extraction of metal ions is the type of acidic medium. The effect of perchloric acid, hydrochloric acid, nitric acid and sulfuric acid on sorption process and complex formation between metal ions and synthesized EIR were studied. For this purpose, 50 mL aliquots of 500 µg L^{-1} U(VI) and Th(IV) solutions (pH 3) were treated with 0.1 g portions of EIR at 298 ± 1 K. As shown in Table 2, the adsorption of metal ions on synthesized EIR with hydrochloric acid gave the highest adsorption percentages. As expected, increasing acid concentration leads to enhance the salt effect and consequently, the adsorption process is encountered with some restriction. Also, the crystals of salt occupy the superficial area of the EIR at high salt concentrations, which diminish the EIR available to interact with the analytes and played a negative role by decreasing the recovery. The same behavior agreed with that reported using other adsorbents [32, 53, 54]. Hydrochloric acid was selected for optimum adsorption experiments.

3.4 Effect of pH

As mentioned above, the synthesized EIR (CAS/XAD-2010) can uptake uranium and thorium in high yield from aqueous hydrochloric acid solutions containing uranium and thorium.

Table 2 The effect of different acid concentrations of several acidic media

Acid conc.	Th adsorption (%)				U adsorption (%)			
	$HClO_4$	HNO_3	HCl	H_2SO_4	$HClO_4$	HNO_3	HCl	H_2SO_4
0.05	93.0	80.0	99.0	73.0	90.3	81.5	99.5	75.2
0.10	78.0	72.2	92.0	61.5	76.6	71.3	87.5	64.6
0.20	64.0	61.0	73.5	50.2	61.5	60.6	70.0	53.8

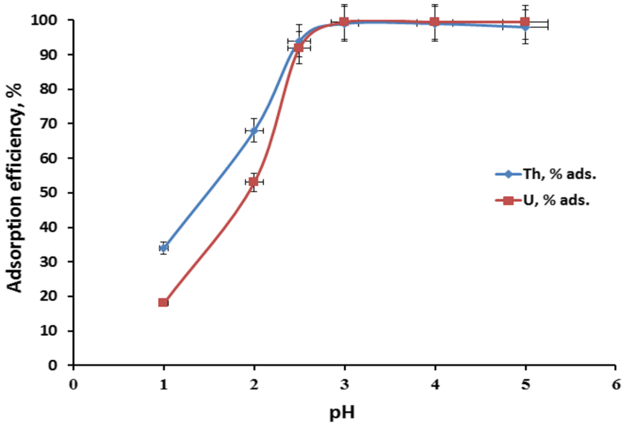

Fig. 3 Effect of pH on the adsorption efficiency percent of uranium and thorium using 50 mL of solution of 0.5 mg L^{-1} with respect to U(VI) and Th(IV) ions

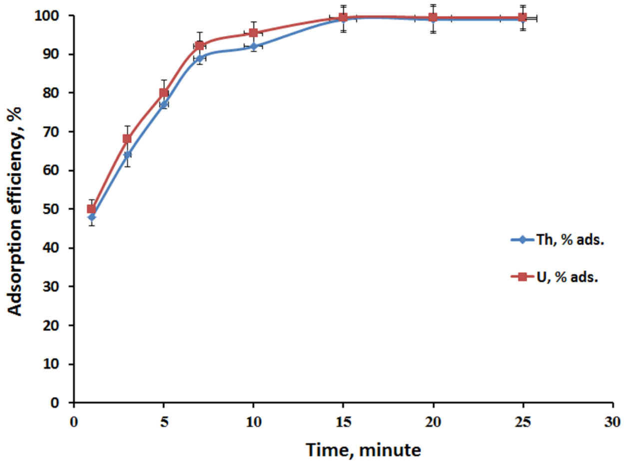

Fig. 4 Effect of time upon uranium and thorium adsorption efficiency from chloride medium by using synthesized EIR

A glance at the extractant structure shows the presence of different donating atoms or functional groups such as OH, C=O, and S-donor ligands which readily form complexes with uranium and thorium ions. The pH extensively affects the metals ion accumulation on the adsorbent and their chelate formation. The effect of pH on the adsorption process was investigated in the range of 1–5 at the above optimum conditions (Fig. 3).

It was found that the adsorption of uranium and thorium were very low using hydrochloric acid solution (0.05 M) with lower pH value. Lower adsorption of each analyte at pH values lower than the optimum values can be due to the rivalry of H^+ with analyte ions for special functional groups, which are responsible for complexation of each analyte to CAS/XAD-2010. In addition, there is the presence of anionic species of these analyte ions at lower pH, which are not adsorbed by EIR. It was noticed that increasing pH led to increase uranium and thorium adsorption efficiency and gave high yield at pH 3–5, may be due to the presence of cationic uranium and thorium species (UO_2Cl^+ and Th^+Cl_3) which is predominate in this region [55–58]. Hence, the pH 3 is selected for the quantitative adsorption of uranium and thorium using the synthesized EIR (CAS/XAD-2010) in the following experiments. The result agreed with that reported earlier using other adsorbents [32, 52, 59–62].

3.5 Effect of Contact Time and Kinetic Studies

Kinetic behavior of uranium and thorium adsorption from 0.05 M hydrochloric acid solution using the synthetic sorbent, in terms of adsorbed amount q_t (mg g^{-1}), is illustrated in Fig. 4. The adsorption into synthesized EIR (CAS/XAD-2010) passes through two stages, the first stage where adsorption increased rapidly up to 7 min. which is attributed to more available sites of EIR for adsorption, and finally equilibrium stage which has been attained at 15 min. Figure 4 referring to all the sites present on adsorbent get satisfied [63, 64]. It can be seen that over 75% of uranium and thorium adsorption efficiency is achieved within the first 5 min. In addition, equilibrium adsorption (99.5% for U and 99% for Th) occurred within 15 min.

The experimental data was treated with various kinetic models including the pseudo-first order and the pseudo-second order for evaluating the kinetic mechanism of adsorption process.

The equations of pseudo-first-order and pseudo-second-order models are specified as follows [65–68]:

$$\log(q_e - q_t) = \log q_e - \frac{k_1 t}{2.303}, \tag{9}$$

$$\frac{t}{q_t} = \frac{1}{k_2 q_e^2} + \frac{t}{q_e}, \tag{10}$$

where q_e and q_t (mg g^{-1}) are the capacities of each analyte adsorption by synthesized EIR at equilibrium and time t respectively. k_1 (1 min^{-1}) and k_2 (g mg^{-1} min^{-1}) are pseudo first-order and second order sorption rate constants, respectively. The values of constants (q_e, k_1, and k_2) were calculated from the lines (Fig. 5) and given in Table 3. Consequently, pseudo second order model has better fitting experimental data performance in terms of higher correlation coefficient and conformity with equilibrium adsorbed amount qe. This suggested the kinetic process is mainly controlled by the chemisorptions which involved chemical bonding between metal ions and the resin active sites.

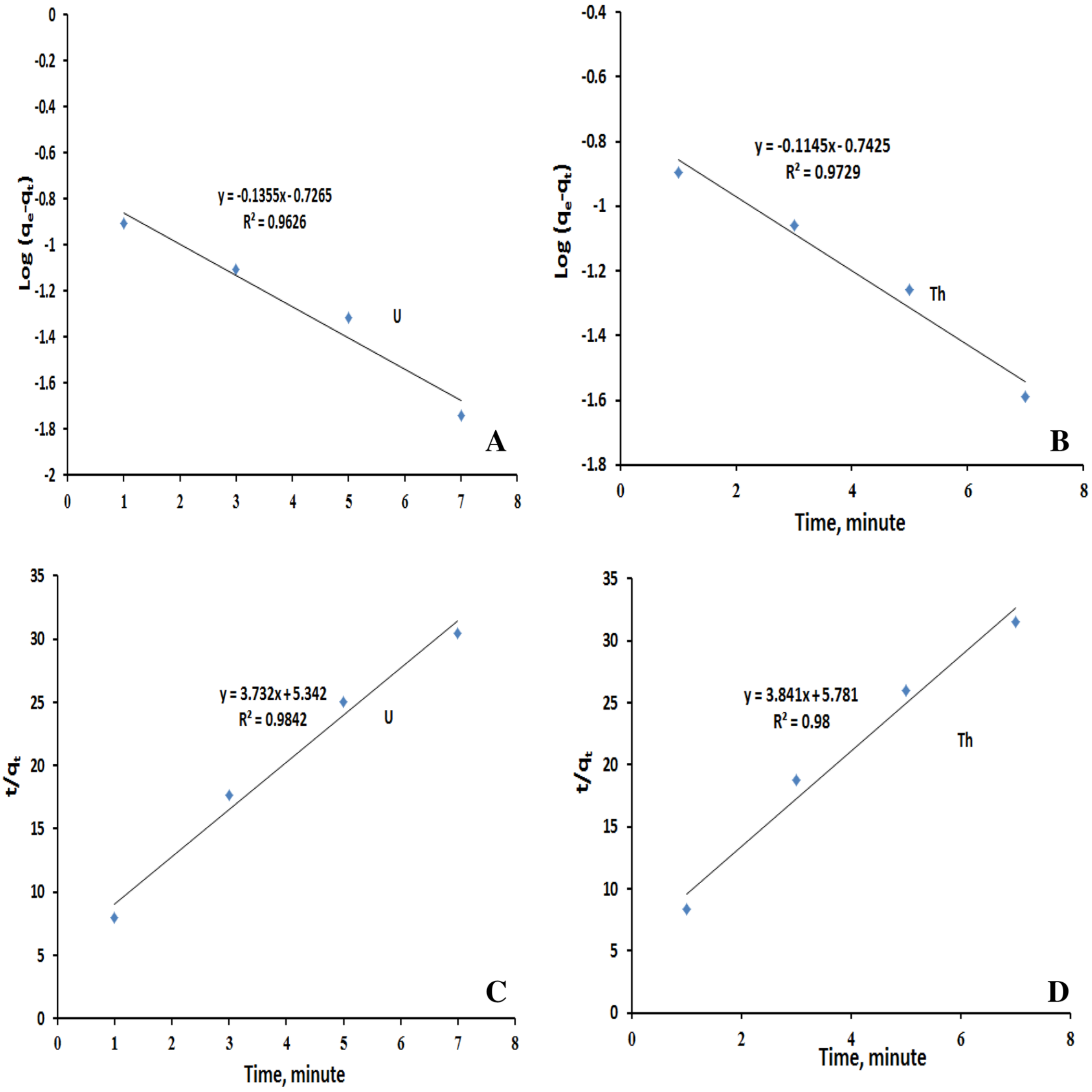

Fig. 5 Pseudo-first-order (**a**, **b**) and pseudo-second (**c**, **d**) kinetics of U and Th adsorption by synthesized EIR from the synthetic hydrochloric acid (0.05 M HCl and 0.5 mg L^{-1} of each U and Th) at 25 °C

Table 3 Kinetic parameters for the adsorption of U(VI) and Th(IV) ions onto synthesized EIR (CAS/XAD-2010)

Metal ions	Exp. q_e (mg g^{-1})	Pseudo-first-order			Pseudo-second-order		
		q_e (mg g^{-1})	K_1 (min^{-1})	R^2	q_e (mg g^{-1})	K_2 (g mg^{-1} min^{-1})	R^2
U(VI)	0.248	0.187	0.312	0.96	0.268	2.61	0.984
Th(IV)	0.247	0.181	0.264	0.97	0.255	2.60	0.980

3.6 Effect of Initial U and Th Concentration and the Adsorption Mechanism

Based on mixing a series of batch experiments at ambient temperature (≈ 25 °C), it can be concluded that the adsorbed uranium and thorium increases with increasing the initial uranium and thorium concentrations in solution till the saturation plateau. The maximum uranium and thorium adsorption capacity was acquired by conducting a fixed EIR (CAS/XAD-2010) weight (0.1 g) with 50 mL of U and Th (at different concentrations) in hydrochloric acid (0.05 M), and at optimum conditions for each metal ion.

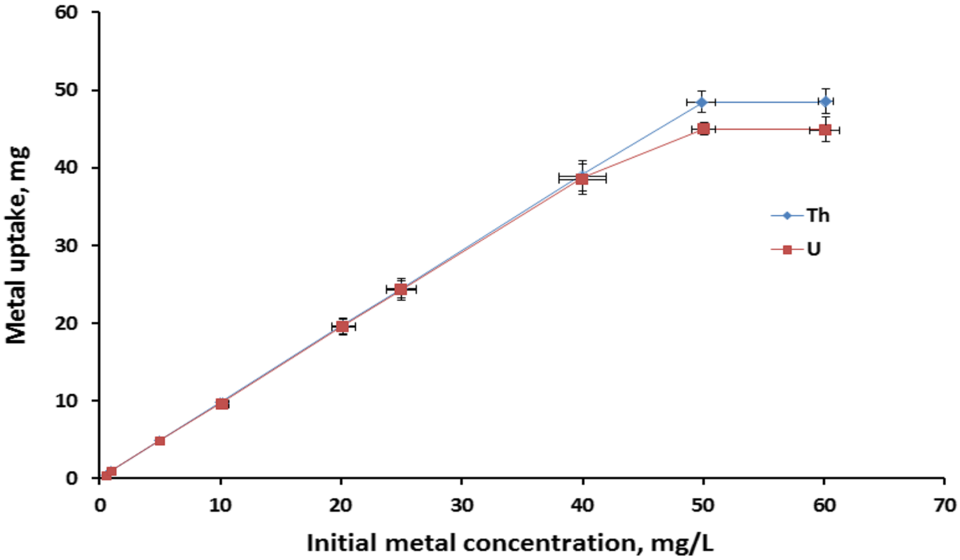

Fig. 6 Effect of initial uranium and thorium concentrations on adsorption efficiency of synthesized EIR from chloride medium

From Fig. 6, we can conclude that the maximum adsorption capacity of uranium and thorium from hydrochloric acid by EIR (CAS/XAD-2010) was 22.5 mg U g^{-1} EIR and 24.25 mg Th g^{-1} EIR. It is interesting to compare the achieved U(VI) and Th(IV) adsorption capacities on the synthesized EIR with other previously prepared adsorbents. It was found that the synthesized EIR is competitive when compared with other previously prepared adsorbents such as modified naphthalene (q_{max} 1.88 mg U g^{-1} [30]), carminic acid (CA) impregnated XAD-16 (1.93 mg U $g^{-1}$and 1.92 mg Th g^{-1} [32]), 3-Hydroxy-2-naphthoic acid/Amberlite XAD-2 (q_{max} 0.047 mmol U g^{-1} and 0.011 mmol Th g^{-1} [47]), Silica modified with rhodamine-B (q_{max} 35 mg U g^{-1} [33]), alizarin red S-impregnated XAD-2010 (q_{max} 20.2 mg U g^{-1} and 18.25 mg Th g^{-1} [47]), CAB/XAD-2010 (q_{max} 156.2 mg U g^{-1} [53]), alizarin red S/Doulite A101 (q_{max} 0.68 mmol U g^{-1} [53]), *N*,*N*-dibutyl-*N*-benzoylthiourea/Amberlite XAD-16 (q_{max} 0.9 mmol U g^{-1} [59]), Mannich type resin (q_{max} 5.2 mg U g^{-1} and 2.28 mg Th g^{-1} [69]), modified benzophenone (q_{max} 2.42 mg U g^{-1} [72] and 1.1 mg Th g^{-1} [70]), Quinoline-8-ol impregnated XAD-4 (q_{max} 2.74 mg U g^{-1} [71]), o-Vaniline semicarbazone impregnated XAD-4 (q_{max} 2.89 U g^{-1} [72]), pyrogallol impregnated XAD-2 (q_{max} 6.71 mg U g^{-1} [73]), modified silica (q_{max} 3.02 mg U g^{-1} [74]), Tiron impregnated XAD-2 (q_{max} 7.70 mg U g^{-1} [75]), and [(2-dihydroxyCASinoylphenylamino) methyl] phosphonic acid functionalized XAD-16 (3.55 mg U $g^{-1}$and 3.25 mg Th g^{-1} [76]).

The infrared technique was used for further study of the adsorption mechanism (Fig. 7). Comparing both spectra of EIR before and after adsorption, it can be observed that; the main difference between absence of thorium and uranium ions (Fig. 2b) and their complexation with impregnated resin (Fig. 7a, b) was the shift if some band which were observed due to interaction with U and Th. The band belonging to C=O unit of synthesized resin was shifted and reduced to 1620 cm^{-1} and 1624 cm^{-1} for Th and U, respectively. Also, the IR spectrum of the modified resin loaded with uranium and thorium were characterized by the shift of C–O bands to 1032 and 1090 cm^{-1}. The band of OH becomes less intense due to the interaction with U and Th ions. The spectra showed new bands of the complexes in the lower frequency range which were assigned as ν(M–O) [77]. As a result, we can say that the ketonic and phenolic groups are coordinated to the U and Th ions and the result agreed with that previously reported [29, 78–82] which indicates that adsorption of uranium and thorium takes place through complexation with CAS loaded on the resin and that Amberlite XAD 2010 is applied only as an immobilization substrate for CAS reagent.

The SEM and EDX images of the CAS/XAD-2010 synthesized resin before and after uranium(VI) and thorium (IV) adsorption are shown in Fig. 8a–c, respectively. From the SEM images it can be clearly observed that there are brilliant spots on the resin beads after U(VI) and Th(IV) adsorption compared to that uniformity and smooth surface of CAS/XAD-2010 synthesized resin before adsorption.

3.7 Isotherm Studies

In order to describe and understand the adsorption properties of uranium and thorium from 0.05 M hydrochloric acid towards synthesized EIR, Langmuir and Freundlich models were established to fit the experimental data. The equation of Langmuir (11) and Freundlich (12) models is specified as follows [81–83]:

$$\frac{C_e}{q_e} = \frac{C_e}{q\text{max}} + \frac{1}{K_L q\text{max}}, \tag{11}$$

Fig. 7 FTIR spectroscopy of Th-loaded synthesized (CAS/XAD-2010) (**a**) and U-loaded synthesized (CAS/XAD-2010) (**b**)

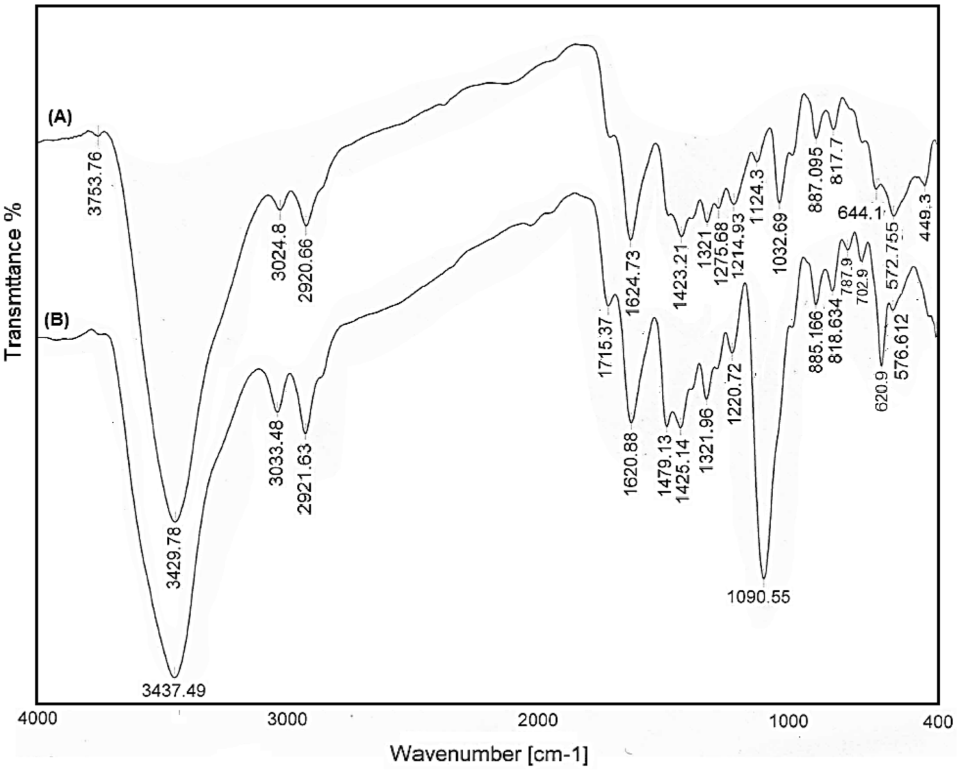

$$\log q_e = \log K_f + \frac{\log C_e}{n}, \tag{12}$$

here, Ce (mg L^{-1}) is the equilibrium concentration of metal in the liquid phase; $q_{\max}$ (mg g^{-1}) is the monolayer capacity in model of Langmuir; K_L (L mg^{-1}) is the Langmuir equilibrium constant; k_f and n are characteristic Freundlich constants related to the relative adsorption capacity of the adsorbent and adsorption intensity, respectively.

The linear plots of (C_e/q_e) vs. C_e for Langmuir isotherm (Fig. 9a, b) or log q_e vs. *log* C_e for Freundlich isotherm (Fig. 9c, d) give the constants of these models, from slope and intercept, which are given in Table 4 and represented adsorption properties of uranium and thorium from 0.05 M hydrochloric acid towards synthesized EIR. Consequently, Langmuir isotherm model has better fitting experimental data performance in terms of higher correlation coefficient and conformity with equilibrium uranium and thorium adsorbed amount from hydrochloric medium. This indicates that monolayer adsorption was the main interaction mechanism of uranyl and thorium ions with the adsorbent.

3.8 Effect of Temperature (Thermodynamics Studies)

For evaluation of the effect of temperature for adsorption of U(VI) and Th(IV) from hydrochloric acid (0.05 M) using synthesized EIR (CAS/XAD-2010), the adsorption process was conducted in a series of batch experiments under various temperatures ranged from 25 to 65 °C. The other parameters were as follows: concentration of each uranium and thorium 0.5 mg L^{-1}, EIR amount 0.1 g, and volume of 50 mL. From Fig. 10, it can be illustrated that heating in the examined range slightly affects the adsorption. Therefore, 25 °C can be considered as the optimum temperature for uranium adsorption experiments.

The thermodynamic parameters of the uranium and thorium adsorption upon EIR synthesized adsorbent have been determined to get an insight into the adsorption behavior of U(VI) and Th(IV) toward EIR. The accurate equilibrium thermodynamic constant (K_e^0) used in Van′t Hoof equation was estimated according to Lima et al. [84]. So, from the obtained results of the best adsorption isotherms (Langmuir model), the equilibrium constants ($K_{isotherm}$) were calculated and their values were converted from L mg^{-1} into L mol^{-1}. Therefore, the k_L (L mol^{-1}) was used in the Van′t Hoof equation, in order to estimate the thermodynamic parameters (ΔH, ΔS, and ΔG) [84]:

$$K_e^0 = K_L/\gamma, \tag{13}$$

$$\ln\left(K_e^0\right) = -\Delta H/RT + \Delta S/R, \tag{14}$$

$$\Delta G = \Delta H - T\Delta S, \tag{15}$$

where K_e^0 (L mol^{-1}) is the thermodynamic equilibrium constant, γ is the coefficient of activity, and the slope

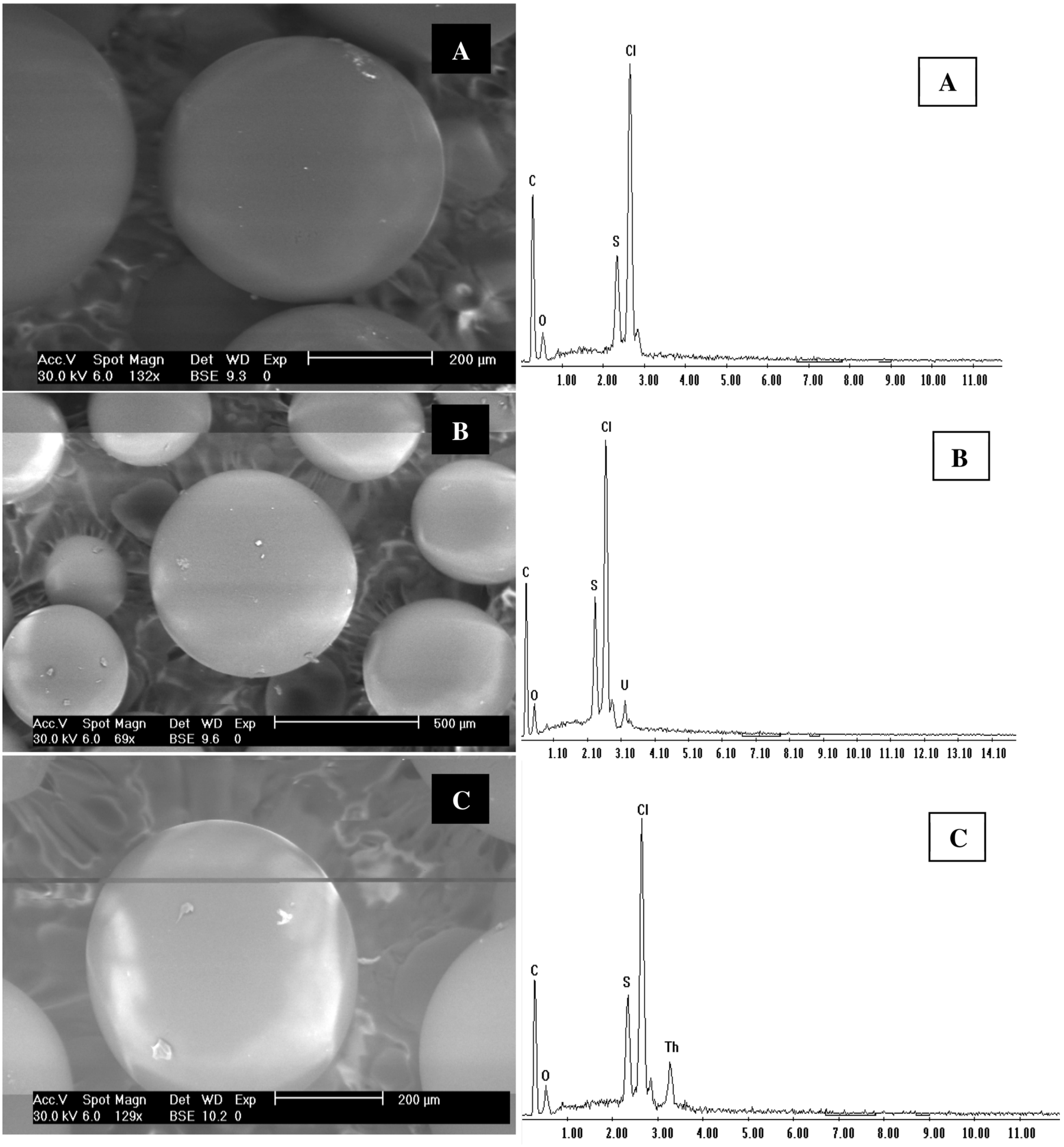

Fig. 8 SEM and EDX images of CAS/XAD-2010 before adsorption (**a**), U-loaded CAS/XAD-2010 (**b**) and Th- loaded CAS/XAD-2010 (**c**)

and intercept of the linear relation between ln K_e^0 and T^{-1} (Fig. 11) were used for calculation of enthalpy (ΔH, kJ mol^{-1}) and entropy (ΔS, J mol^{-1} K^{-1}) respectively. The negative value of ΔH (− 12.49 kJ mol^{-1} for U and − 12.47 kJ mol^{-1}for Th) indicated that the adsorption process of U(VI) and Th(IV) by EIR was an exothermic reaction. The values of ΔS are 66.05 J mol^{-1} K^{-1} for U and 67.62 J mol^{-1} K^{-1} for Th. Negative Gibbs free energy ΔG value (− 32.17 kJ mol^{-1} for U and − 32.63 kJ mol^{-1} for Th) demonstrated the spontaneous property of this adsorption [47, 85–87].

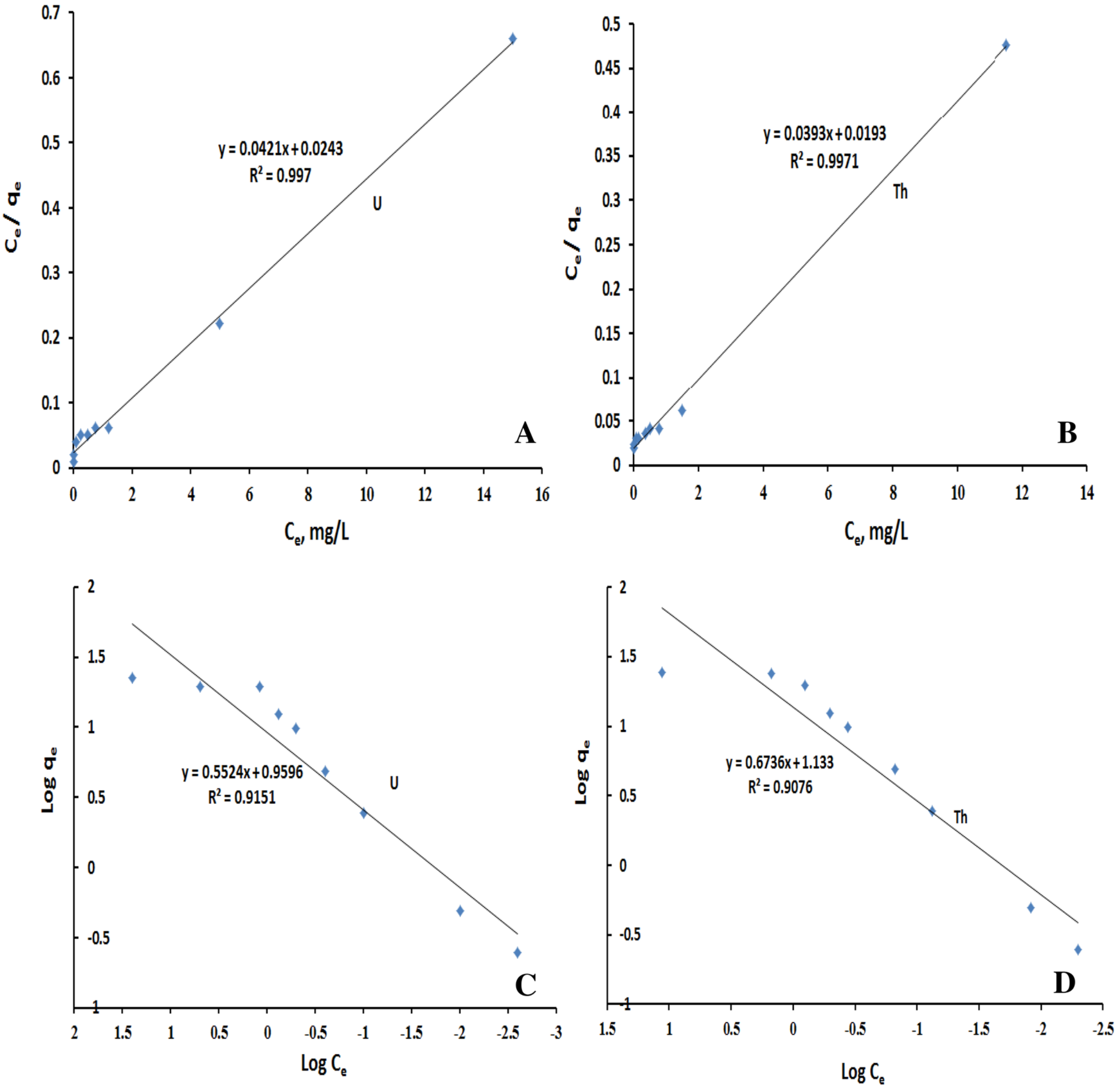

Fig. 9 Langmuir (**a**, **b**) and Freundlich (**c**, **d**) models of U and Th adsorption by synthesized EIR

Table 4 Isotherm parameters for the adsorption of U(VI) and Th(IV) ions onto synthesized EIR (CAS/XAD-2010)

Metal ions	Exp. $q_{\max}$ (mg g^{-1})	Langmuir parameters			Freundlich parameters		
		q_{max} (mg g^{-1})	K_L (L mg^{-1})	R^2	n	Kf	R^2
U(VI)	22.50	23.8	1.733	0.997	1.81	9.11	0.915
Th(IV)	24.25	25.44	2.04	0.997	1.48	13.58	0.907

3.9 Interference Effect

The interference effect was necessary to be studied for spectrophotometric determination of thorium and uranium in different geological rock samples. Some of the common cations associated with studied metals and may show adsorption behavior on the CAS-modified resin and interferes during their spectrophotometric determination namely, Na^+, K^+, Ca^{2+}, Mg^{2+}, Al^{3+}, Mn^{2+}, Fe^{3+}, Cr^{6+}, VO^{2+}, Cu^{2+}, Co^{3+}, Sr^{2+}, Ln^{3+}, NO_3^-, SO_4^{2-}, PO_4^{3-}, and HCO_3^-.

In the present experimental section, the effect of the above listed cations was studied by adding different volumes from their working solutions to a constant uranium and thorium (1 µg mL^{-1}) concentration. The absorbances of these mixtures were measured in aqueous solutions after contacting with CAS/XAD-2010 adsorbent at the optimized studied conditions. From the obtained results (Table 5), it was found

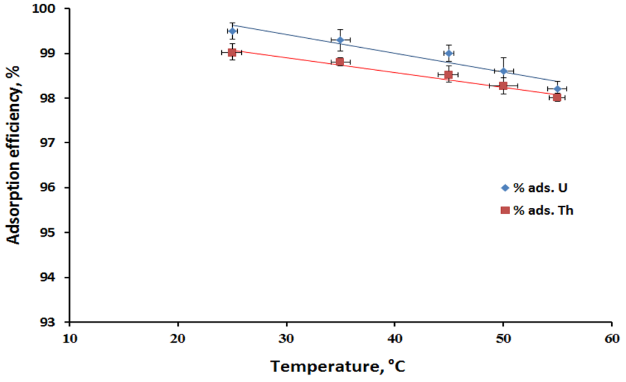

Fig. 10 Effect of temperature on the adsorption efficiency of uranium and thorium using synthesized EIR (CAS/XAD-2010) adsorbent (adsorption condition: 50 ml 0.5 mg L of each uranium and thorium ions solution (pH 3), 0.05 M hydrochloric acid, 0.1 g EIR, 15 min contact time)

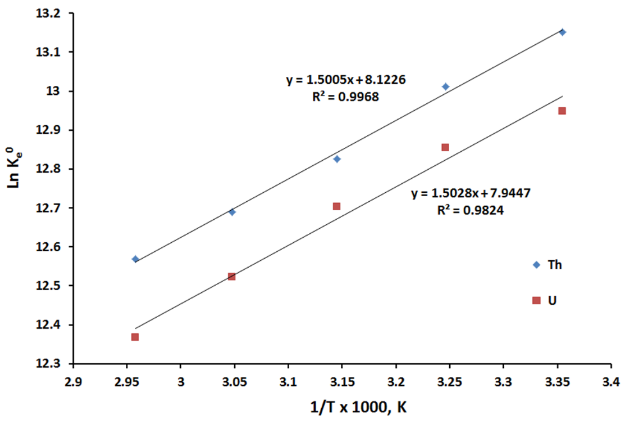

Fig. 11 The plot of Ln K_e^0 versus 1/T of the uranium and thorium adsorption upon synthesized EIR (adsorption condition: 50 mL 0.5 mg L^{-1} of each uranium and thorium ions solution (pH 3), 0.05 M hydrochloric acid, 0.1 g EIR, 15 min contact time)

that; the synthesized CAS/XAD-2010 adsorbent gives high tolerance limit and emphasizes the selective adsorption of uranium and thorium from hydrochloric acid medium.

Table 5 Effect of foreign ions on the adsorption of uranium and thorium from hydrochloric solution with equal concentration of 1 μg mL^{-1} for both analytes

Metal ion	Tolerance ratio	
	Th(IV)	U(VI)
Ca^{2+}	5000	4000
Mg^{2+}	5000	4000
Na^{+}	5000	4000
K^{+}	5000	4000
Sr^{2+}	5000	4000
Al^{3+}	5000	4000
Mn^{2+}	5000	4000
Fe^{3+}	200	200
Co^{2+}	700	700
Cu^{2+}	700	700
Zn^{2+}	700	700
Cd^{2+}	700	700
VO^{2+}	500	500
Ni^{2+}	500	500
Pb^{2+}	500	500
Ln^{3+}	100	100
Zr^{4+}	100	100
NO_3^{-}	5000	5000
SO_4^{2-}	3000	3000
PO_4^{3-}	950	950
HCO_3^{-}	900	900

3.10 Adsorption Mechanism

The adsorbent chemical composition plays an important role in expressing the adsorption mechanism. Several possible reactions may interfere for the removal of metal ions by adsorption, from such actions are acid–base interactions, ion exchange, coordination/chelation, complexation, precipitation, physical adsorption, and electrostatic interactions. FTIR, SEM, EDX and elemental analysis techniques are most widely used to understand the mechanism of adsorption. Usually, the hydroxyl and carboxyl functional groups seem to be the major routes for the adsorption of U and Th. The adsorption of U and Th can occur mostly by complexation with the mentioned functional groups. The involvement of these groups could be attributed by shift of FTIR peaks as shown in Fig. 7. In many cases, the pH dependent adsorption studies have followed a very similar pattern where initially, the adsorption performance of the adsorbent increased with the increase in the pH value, reached a maximum at a certain pH, and then decreased at higher pH [15, 16]. This trend has been explained by considering the electrostatic interaction between the surface of the adsorbent and the metal ion species at a particular pH. At lower pH (Fig. 3), the surface remained positively charge due to protonation of the functionalities [60] and no appreciable sorption of metal ion was observed because of the electrostatic repulsion between the metal ion and the positively charged surface. A gradual increase in the pH favored the adsorption as a shift in the surface charge from positive to negative led to the electrostatic attraction between the metal ions and the surface of the adsorbent and form high stable complexes through the ionizable hydroxyl and adjacent carboxylate groups [24]. With regards to Langmuir adsorption constant calculated for each one of the metal ions, it is approved that the adsorption can be carried out via a chemisorption process according to the following equations:

$$\overline{2(H_2CA)} + UO_2^{2+} \rightleftarrows \overline{(HCA)_2UO_2} + 2H^+, \tag{16}$$

$$\overline{2(H_2CA)} + Th^{4+} \rightleftarrows \overline{(CA)_2Th} + 4H^+, \tag{17}$$

Table 6 Effect of different eluting agents concentrations upon U(VI) and Th(IV) from the loaded EIR

Reagent conc. (M)	Th elution (%)			U elution (%)		
	$(NH_4)_2CO_3$	HCl	$NH_4H_2PO_4$	$(NH_4)_2CO_3$	HCl	$NH_4H_2PO_4$
0.5	12.0	43.8	1.0	33.7	38.5	54.0
1.0	20.6	99.5	1.5	68.0	65.0	99.6
2.0	22.5	99.5	1.9	70.2	71.6	99.6

where the bar denotes the species in the organic phase of the impregnated resin and H_2CA is the acidic form of it.

3.11 Elution Studies

Quantitative desorption of U(VI) and Th(IV) was performed with various eluting agents such as hydrochloric acid, ammonium dihydrogen phosphate, ammonium carbonate, and hydrochloric acid which form stable complexes with uranium and thorium [32, 54, 69, 87, 88]. For this purpose, 10 mL aliquots of each eluting agent with various concentrations were treated with 0.1 g portions of loaded EIR at 298 ± 1 K for 10 min. From Table 6, we can conclude that the maximum elution efficiency (99.6%) of uranium was achieved by 1 M ammonium dihydrogen phosphate while, the maximum elution efficiency (99.5%) of thorium was achieved by 1 M HCl. From these results the selective elution of uranium over thorium was achieved.

3.12 EIR Reusability

The EIR reusability was checked by subjecting the synthesized EIR (CAS/XAD-2010) to several loading and elution experiments. The capacity of the synthesized EIR (CAS/XAD-2010) was found to be practically constant (variation < 1%) after its repeated use for more than 50 runs, thus indicating the multiple use of EIR is feasible.

3.13 Application of Proposed Method on Standard Geological and Granitic Samples

The proposed method was applied for preconcentration and determination of U(VI) and Th(IV) in different samples including international reference and geological samples to verify its applications and validations. The samples were firstly decomposed by Afifi et al. and Fouad et al. [89, 90] to overcome the high concentration of major oxides. The

Table 7 Comparison of uranium and thorium concentrations in standard reference rock samples and the present studied method

Standard sample	Certified value (ppm)	Concentration of U, Th found using present method (ppm)	S.D.	S.E.	Error (%)	Accuracy
DL-1a[a]	76 Th	76.3	0.36	0.208	0.27	±0.36
		75.6				
		75.8				
	116 U	115.5	0.21	0.12	0.106	±0.208
		115.6				
		115.9				
DH-1a[a]	91Th	91.2	0.23	0.135	0.148	±0.23
		90.8				
		91.8				
	2629 U	2627.5	0.32	0.186	0.007	±0.32
		2626.9				
		2627.0				
Nim.G[b]	51 Th	51.3	0.36	0.208	0.408	±0.25
		50.8				
		50.6				
	15 U	15.4	0.21	0.12	0.804	±0.306
		14.8				
		15.2				

[a] Certified values reported by Canadian Central for Mineral and Energy Technology standards (CANMET), certifying agency

[b] Certified values reported by SA Bureau of standards P/Bag X191, Pretoria 0001 (SARM1)

S.D standard deviation, *S.E* standard error

Table 8 Comparison between uranium and thorium concentrations in the granitic rock samples using the present method

Granitic sample ID	Expected U, Th concentration (ppm)[a]	Concentration of U, Th found using present method (ppm)	S.D.	S.E.	Error (%)	Accuracy
M50	167.2 Th	167.2	0.306	0.176	0.106	±0.305
		166.8				
		167.4				
	49 U	49.0	0.21	0.12	0.248	±0.208
		48.7				
		48.6				
M57	93.9 Th	93.8	0.152	0.088	0.09	±0.153
		93.9				
		93.6				
	24 U	24.0	0.30	0.174	0.72	±0.30
		24.4				
		23.8				
T77	115 Th	115.5	0.252	0.145	0.126	±0.251
		115.8				
		115.3				
	30 U	30.0	0.20	0.11	0.38	±0.20
		29.6				
		29.8				
T78	81.3 Th	81.3	0.45	0.26	0.319	±0.451
		80.8				
		81.7				
	60 U	67.8	0.29	0.166	0.247	±0.288
		67.3				
		67.3				

[a] Analyzed by ICP-OES and Laser fluorometer

serious interference from above studied cations was avoided by masking with potassium cyanide (1×10^{-3} M) [91], Then, uranium and thorium was separated from acidic solutions using synthesized EIR (CAS/XAD-2010) adsorbent at the optimum studied conditions and analyzed in the eluted solutions spectrophotometrically with good accuracy (Tables 7 and 8). Thus, these results indicated that the proposed method is accurate, simple and cost-effective for analyzing studied samples containing uranium and thorium.

4 Conclusions

A combination between separation of U(VI) and Th(IV) ions by a high stable EIR and spectrophotometric determination was described. The new EIR was prepared by impregnating chrome azurol S onto Amberlite XAD-2010 beads. The maximum adsorption capacity with respect to interested metal ions was acquired by contacting a fixed EIR (CAS/XAD-2010) weight (0.1 g) with 50 mL of each uranium and thorium ions solution (pH 3) in hydrochloric acid (0.05 M) for 15 min contact time at room temperature. Langmuir isotherm model has the best fitting experimental data with a maximum adsorption capacity of 23.8 mg g^{-1} for U(VI) and 25.44 mg g^{-1} for Th(IV). The adsorption process of each metal ion by synthesized chrome azurol S-impregnated XAD-2010 showed an exothermic pseudo-second-order adsorption process. The loaded metal ions were selectively eluted using 1 M of 10 mL HCl solution for Th(IV) and 1 M of 10 mL ammonium dihydrogen phosphate solution for U(VI) using 10 min contact time. The tolerance limits for several metal ions on chrome azurol S-impregnated XAD-2010 were calculated and gave high tolerance limit. The optimized method was applied to reference and different rock types bearing thorium and uranium with good accurate results.

Compliance with ethical standards

Conflict of interest On behalf of all authors, the corresponding author states that there is no conflict of interest.

References

1. Agency for Toxic Substances and Disease Registry, US Public Health Service, New York (2008) Health consultation. Depleted uranium at Hawaiian military sites; Schofield Barracks Impact Area; Makua Military Reservation, Pohakuloa Training Area on Islands of Oahu and Hawaii
2. Jain V, Pandya R, Pillai S, Shrivastav P (2006) Solid phase extraction, preconcentration and sequential separation of U(VI), Th(IV), La(III) and Ce(III) by octa-*O*-methoxy resorcin[4]arene based amberlite XAD-4 chelating resin. Talanta 70:257–266. https://doi.org/10.1016/j.talanta.2006.02.032
3. Welz B, Sperling M (1999) Atomic absorption spectrometry. Wiley-VCH, New York
4. Tamborini G (2004) SIMS analysis of uranium and actinides in microparticles of different origin. Microchim Acta 145:237–242. https://doi.org/10.1007/s00604-003-0160-8
5. Dean J (1997) Atomic absorption and plasma spectroscopy. Wiley, London
6. Marczenko Z, Balcerzak M (2000) Separation, preconcentration and spectrophotometry in inorganic analysis, vol 10. Elsevier, Amsterdam
7. Perkampus H (1992) UV–Vis spectroscopy and its applications. Springer-Verlag, Berlin, p 33
8. Pretty J, Van Berkel G, Duckworth D (1998) Adsorptive stripping voltammetry as a sample pretreatment method for trace uranium determinations by inductively coupled plasma mass spectrometry. Int J Mass Spectrom 178:51–63. https://doi.org/10.1016/S1387-3806(98)80001-8
9. Dojozan D, Pournaghi-Azar M, Toutounchi-Asr J (1998) Preconcentration of trace uranium from seawater with solid phase extraction followed by differential pulse polarographic determination in chloroform eluate. Talanta 46:123–128. https://doi.org/10.1016/S0039-9140(97)00252-X
10. Miura T, Morimoto T, Hayano K, Kishimoto T, Kagaku P (2000) Determination of uranium in water samples by ICP-AES with chelating resin disk preconcentration. Bunseki Kagaku 49:245–249. https://doi.org/10.2116/bunsekikagaku.49.245
11. Kato K, Ito M, Watanabe K (2000) Determination of thorium and uranium in activated concrete by inductively coupled plasma mass spectrometry after anion-exchange separation. Fresenius' J Anal Chem 366:54. https://doi.org/10.1007/s002160050011
12. Torgov V, Demidova M, Saprykin A, Nikolaeva I, Us T, Chebykin E (2002) Extraction preconcentration of uranium and thorium traces in the analysis of bottom sediments by inductively coupled plasma mass spectrometry. Anal Chem 57:303. https://doi.org/10.1023/A:1014942112864
13. Sengupta A, Ippili T, Jayabun S, Singh M, Thulasidas K (2016) ICP-AES determination of trace metallic constituents in thorium matrix after preferential extraction of thorium using TBP, TOPO and DHOA: a comparative study. J Radioanal Nucl Chem 310(1):59–67. https://doi.org/10.1007/s10967-016-4790-9
14. Amer T, El-Sheikh E, Hassanin M, Fathy W (2019) Processing of monazite mineral concentrate for selective recovery of uranium. Chem Afr 2:123. https://doi.org/10.1007/s42250-018-00037-8
15. Gupta N, Sengupta A, Gupta A, Sonawane J, Sahoo H (2018) Biosorption—an alternative method for nuclear waste management: a critical review. J Environ Chem Eng 6(2):2159–2175. https://doi.org/10.1016/j.jece.2018.03.021
16. Sengupta A, Gupta N (2017) MWCNTs based sorbents for nuclear waste management: a review. J Environ Chem Eng 5(5):5099–5114. https://doi.org/10.1016/j.jece.2017.09.054
17. Zhang T, Shan X, Liu R, Tang H, Zhang S (1998) Preconcentration of rare earth elements in seawater with poly(acrylaminophosphonic dithiocarbamate) chelating fiber prior to determination by inductively coupled plasma mass spectrometry. Anal Chem 70:3964–3968. https://doi.org/10.1021/ac980321h
18. Tolmachyov S, Kuwabara J, Noguchi H (2004) Flow injection extraction chromatography with ICP-MS for thorium and uranium determination in human body fluids. J Radioanal Nucl Chem 261:125. https://doi.org/10.1023/B:JRNC.0000030945.53499.1c
19. Ghaedi M, Fathi M, Shokrollahi A, Shajarat F (2006) Highly selective and sensitive preconcentration of mercury ion and determination by cold vapor atomic absorption spectroscopy. Anal Lett 39:1171–1185. https://doi.org/10.1080/00032710600622167
20. Ghaedi M, Asadpour E, Vafaie A (2006) Simultaneous preconcentration and determination of copper, nickel, cobalt, lead and iron content using a surfactant coated alumina. Bull Chem Soc Jpn 79:432–436. https://doi.org/10.1246/bcsj.79.432
21. Baytak S, Balaban A, Turker A, Erk B (2006) Atomic absorption spectrometric determination of Fe(III) and Cr(III) in various samples after preconcentration by solid-phase extraction with pyridine-2-carbaldehyde thiosemicarbazone. J Anal Chem 61:476. https://doi.org/10.1134/S106193480605008X
22. Lemos V, David G, Santos L (2006) Synthesis and application of XAD-2/Me-BTAP resin for on-line solid phase extraction and determination of trace metals in biological samples by FAAS. J Braz Chem Soc 17:697–704. https://doi.org/10.1590/S0103-50532006000400010
23. Korn M, Santos A, Jaegera H, Silva N, Costa A (2004) Copper, zinc and manganese determination in saline samples employing FAAS after separation and preconcentration on amberlite XAD-7 and Dowex 1X-8 Loaded with Alizarin Red S. J Braz Chem Soc 15(2):212–218
24. Hosseini M, Bazrafshan A, Hosseini-Bandegharaei A (2016) A novel solvent-impregnated resin containing 3-hydroxy-2-naphthoic acid for stepwise extraction of Th(IV) and U(VI) over other coexistence ions. Sep Sci Technol 51(8):1328–1335. https://doi.org/10.1080/01496395.2016.1147465
25. Dubey R, Bhalotra A, Gupta M, Puri B (1998) Differential-pulse polarographic-determination of uranium (VI) in standard and synthetic samples after adsorption of its quinolin-8-olate on microcrystalline naphthalene. Anal Chim 88:719–729
26. Seki T, Oguma K (2004) Determination of uranium in natural waters and high-purity aluminum by flow-injection on-line preconcentration and ICP-MS detection. Bunseki Kagaku 53:353–357. https://doi.org/10.2116/bunsekikagaku.53.353
27. Rao T, Metilda P, Mary Gladis J (2006) Preconcentration techniques for uranium(VI) and thorium(IV) prior to analytical determination—an overview. Talanta 68:1047–1064. https://doi.org/10.1016/j.talanta.2005.07.021
28. Pyrzy˜nska K, Trojanowicz M (1999) Functionalized cellulose sorbents for preconcentration of trace metals in environmental analysis. Crit Rev Anal Chem 29:313–321. https://doi.org/10.1080/10408349891199329
29. Ghaedi M, Niknam K, Zamani S, Larki H, Roosta M, Soylak M (2013) Silica chemically bonded *N*-propyl kriptofix 21 and 22 with immobilized palladium nanoparticles for solid phase extraction and preconcentration of some metal ions. Mater Sci Eng C 33:3180–3189. https://doi.org/10.1016/j.msec.2013.03.045
30. Gladis J, Rao T (2002) Solid phase extractive preconcentration of uranium on to 5,7-dichloroquinoline-8-ol modified naphthalene. Anal Lett 35:501–515. https://doi.org/10.1081/AL-120002683
31. Hosseini M, Hosseini-Bandegharaei A (2011) Comparison of sorption behavior of Th(IV) and U(VI) on modified impregnated resin containing quinizarin with that conventional prepared impregnated resin. J Hazard Mater 190:755–765. https://doi.org/10.1016/j.jhazmat.2011.03.111

32. Hosseini-Bandegharaei A, Hosseini M, Jalalabadi Y, Nedaie M, Sarwghadi M, Taherian A, Hosseini E (2011) A novel extractant-impregnated resin containing carminic acid for selective separation and pre-concentration of uranium(VI) and thorium(IV). Int J Environ Anal Chem 93:108–124. https://doi.org/10.1080/03067319.2011.620706
33. Ali A, Nouh E (2019) Rhodamine-B modified silica for uranium (VI) extraction from aqueous waste samples. Sep Sci Technol 54(4):602–614. https://doi.org/10.1080/01496395.2018.1512620
34. Soylak M, Elci L, Dogan M (2001) Solid Phase extraction of trace metal ions with amberlite XAD resins prior to atomic absorption spectrometric analysis. J Trace Microprobe Technol 19:329–344. https://doi.org/10.1081/TMA-100105049
35. Lemos V, Nunes L, Baliza P, Santos J, Yamaki R, Jesus A (2004) On-line solid phase extraction system for cadmium preconcentration and determination by flame atomic absorption spectroscopy. Can J Anal Sci Spectrosc 49:24–30
36. Qadeer R, Hanif J, Khan M, Saleem M (1995) Uptake of uranium ions by molecular sieve. Radiochim Acta 68(3):197–201. https://doi.org/10.1524/ract.1995.68.3.197
37. Landgraf W, Li N, Benson J (2003) Polymer microcarrier exhibiting zero-order release. Drug Delivery Technol 3:1–12
38. Sigma-Aldrich (2006) Amberlite XAD polimeric resins. http://www.sigmaaldrich.com/sigma/product%20information%20sheet/xad7pis.pdf. Accessed 10 Aug 2006
39. Bulut V, Duran C, Tufekci M, Elci L, Soylak M (2007) Speciation of Cr(III) and Cr(VI) after column solid phase extraction on Amberlite XAD-2010. J Hazard Mater 143:112–117. https://doi.org/10.1016/j.jhazmat.2006.08.074
40. Duran C, Gundogdu A, Bulut V, Soylak M, Elci L, Senturk H, Tufekci M (2007) Separation and enrichment of gold (III) from environmental samples prior to its flame atomic absorption spectrometric determination. J Hazard Mater 149:317–323. https://doi.org/10.1016/j.jhazmat.2007.03.083
41. Duran C, Senturk H, Gundogdu A, Bulut V, Elci L, Soylak M, Tufekci M, Uygur Y (2007) Determination of some trace metals in environmental samples by flame AAS following solid phase extraction with amberlite XAD-2000 resin after complexing with 8-hydroxyquinoline. Chin J Chem 25:196–202. https://doi.org/10.1002/cjoc.200790040
42. Hosseini M, Hosseini-Bandegharaei A (2010) Selective extraction of Th(IV) over U(VI) and other co-existing ions using eosin B impregnated Amberlite IRA-410 resin beads. J Radioanal Nucl Chem 283:23–30. https://doi.org/10.1007/s10967-009-0037-3
43. Hosseini M, Hosseini-Bandegharaei A, Raissi H et al (2009) Sorption of Cr(VI) by Amberlite XAD-7 resin impregnated with brilliant green and its determination by quercetin as a selective spectrophotometric reagent. J Hazard Mater 169:52–57. https://doi.org/10.1016/j.jhazmat.2009.03.058
44. Hosseini M, Hosseini-Bandegharaei A, Hosseini M (2009) Column-mode separation and pre-concentration of some heavy metal ions by solvent-impregnated resins containing quinizarin before the determination by flame atomic absorption spectrometry. Int J Environ Anal Chem 89:35–48. https://doi.org/10.1080/03067310802464948
45. Hosseini-Bandegharaei A, Hosseini M, Jalalabadi Y (2011) Removal of Hg(II) from aqueous solutions using a novel impregnated resin containing 1-(2-thiazolylazo)-2-naphthol (TAN). Chem Eng J 168:1163–1173. https://doi.org/10.1016/j.cej.2011.02.004
46. Hosseini-Bandegharaei A, Hosseini M, Sarw-Ghadi M, Zowghi S, Hosseini E, Hosseini-Bandegharaei H (2010) Kinetics, equilibrium and thermodynamic study of Cr(VI) sorption into toluidine blue o-impregnated XAD-7 resin beads and its application for the treatment of wastewaters containing Cr(VI). Chem Eng J 160:190–198. https://doi.org/10.1016/j.cej.2010.03.040
47. Fouad H, Elenein SA, Orabi A, Abdulmoteleb S (2019) A new extractant impregnated resin for separation of traces of uranium and thorium followed by their spectrophotometric determination in some geological samples. SN Appl Sci 1:309. https://doi.org/10.1007/2Fs42452-019-0325-7
48. Marczenko Z (1986) Separation and spectrophotometric determination of elements, vol 60. Wiley, New York
49. Leenheer A, Ruyter M, Steyaert H (1976) A method for the statistical evaluation of results in external quality control surveys. Clin Chim Acta 71:229–238. https://doi.org/10.1016/0009-8981(76)90535-0
50. Davis J (1986) Handbook of statistics and analysis in geology, 2nd edn. Wiley, New York
51. Christian G (1994) Handbook of analytical chemistry, Chapter 2, 5th edn. Wiley, New York, pp 22–26
52. Maihub A, El-ajaily M, Aboukrish M (2003) Synthesis and characterization of some homodinuclear mixed ligand complexes of Co(II) and Cu(II) part II. Jerash Res Stud 7(2):41–47
53. Hosseini-Bandegharaei A, Sarwghadi M, Heydarbeigi A, Hosseini S, Nedaie M (2013) Solid-phase extraction of trace amounts of uranium(VI) in environmental water samples using an extractant-impregnated resin followed by detection with UV–Vis spectrophotometry. J Chem 2013:1–10. https://doi.org/10.1155/2013/671564
54. Hosseini S, Rahmani-Sani A, Jalalabadi Y, Karimzadeh M, Hosseini-Bandegharaei A, Kharghani K, Allahabadi A (2015) Preconcentration and determination of ultra-trace amounts of U(VI) and Th(IV) using titan yellow impregnated Amberlite XAD-7 resin. Int J Environ Anal Chem 95:277–290. https://doi.org/10.1080/03067319.2015.1016009
55. Cheira M, Orabi A, Hassanin M, Hassan S (2018) Chem Data Collect 13–14:84–103. https://doi.org/10.1016/j.cdc.2018.01.003
56. Barbano P, Rigali L (1978) Anal Chim Acta 96(1):199–201
57. Sato T (1983) Hydrometallurgy 22:121–140
58. Jha M, Kumar V, Singh R (2002) Solvent Extr Ion Exch 20(3):389–405
59. Merdivan M, Zahir Z, Hamamci C (2001) Sorption behaviour of uranium(VI) with *N*,*N*-dibutyl-*N*-benzoylthiourea impregnated in amberlite XAD-16. Talanta 55:639–645
60. Upase A, Zade A, Kalbende P (2011) Spectrophotometric microdetermination of thorium(IV) and uranium(VI) with chrome azurol-S in presence of cationic surfactant. E J Chem 8(3):1132–1141
61. Bursali E, Merdivan E, Yurdakoc M (2010) Preconcentration of uranium(VI) and thorium(IV) from aqueous solutions using low-cost abundantly available sorbent. J Radioanal Nucl Chem 283:471–476. https://doi.org/10.1007/s10967-009-0365-3
62. Khalifa M (1998) Selective separation of uranium using alizarin red S (ARS)-modified anion-exchange resin or by flotation of U-ARS chelate. Sep Sci Technol 33:2123–2141. https://doi.org/10.1080/01496399808545719
63. Mishra S, Achary G, Das M (2012) Adsorption of Cu(II) by used aqua guard carbon(UAC). J Chem Pharm Res 4(2):1207–1216
64. Sharma I, Goyal D (2009) Kinetic modeling: chromium(III) removal from aqueous solution bymicrobial waste biomass. J Sci Ind Res 68:640–646
65. Ho Y, McKay G (1999) Pseudo-second order model for sorption processes. Process Biochem 34:451–465. https://doi.org/10.1016/S0032-9592(98)00112-5
66. Lagergren S (1898) About the theory of so-called adsorption of soluble substance. Kungliga Svenska Vetenskapsakademiens Handlingar 24:1–39
67. Hosseini-Bandegharaei A, Khamirchi R, Hekmat-Shoar R, Rahmani-Sani A, Rastegar A, Pajohankia Z, Fattahi Z (2016) Sorption efficiency of three novel extractant-impregnated resins containing vesuvin towards Pb(II) ion: effect of nitrate and amine

functionalization of resin backbone. Coll Surf A Physicochem Eng Aspects. https://doi.org/10.1016/j.colsurfa.2016.05.060

68. Hosseini-Bandegharaei A, Alahabadi A, Rahmani-Sani A, Rastegar A, Khamirchi R, Mehrpouyan M, Agah J, Pajohanki Z (2016) Effect of nitrate and amine functionalization on the adsorption properties of a macroporous resin towards tetracycline antibiotic. J Taiwan Inst Chem Eng 66:143–153
69. Elsalamouny A, Desouky O, Mohamed S, Galhoum A (2016) Evaluation of adsorption behavior for U(VI) and Th(IV) ions onto solidified Mannich type material. J Dispersion Sci Technol 38:860–865. https://doi.org/10.1080/01932691.2016.1207546
70. Preetha C, Gladis J, Rao T (2002) Solid phase extractive preconcentration of thorium onto 5,7-dichloroquinoline-8-ol modified benzophenone. Talanta 58:701–709. https://doi.org/10.1016/S0039-9140(02)00378-8
71. Gladis J, Rao J (2002) Quinoline-8-ol-immobilized Amberlite XAD-4: synthesis, characterization, and uranyl ion uptake properties suitable for analytical applications. Anal Bioanal Chem 373:867–887. https://doi.org/10.1007/s00216-002-1387-7.12194052
72. Jain V, Handa A, Sait S, Shrivastav P, Agrawal Y (2001) Pre-concentration, separation and trace determination of lanthanum(III), cerium(III), thorium(IV) and uranium(VI) on polymer supported o-vanillinsemicarbazone. Anal Chim Acta 429:237–246. https://doi.org/10.1016/S0003-2670(00)01299-X
73. Kumar M, Rathore D, Singh A (2001) Pyrogallol immobilized Amberlite XAD-2: a newly designed collector for enrichment of metal ions prior to their de-termination by flame atomic absorption spectrometry. Mikrochim Acta 137:127–134. https://doi.org/10.1007/s006040170002
74. Jal P, Dutta R, Sudershan K, Saha M, Bhattacharya A, Chintalapudi S, Mishra B (2001) Extraction of metal ions using chemically modified silica gel: a PIXE analysis. Talanta 55:233–240. https://doi.org/10.1016/S0039-9140(00)00678-0
75. Kumar M, Rathore D, Singh A (2000) Metal ion enrichment with Amberlite XAD-2 functionalized with Tiron: analytical applications. Analyst 125:1221–1226. https://doi.org/10.1039/b000858n
76. Hosseini M, Hosseini M, Bandeh-Gharaei A (2007) Solvent Impregnated resins containing quinizarin: preparation and application to batch-mode separation of Cd(II), Cu(II), Ni(II), and Zn(II) in aqueous media prior to the determination by flame atomic absorption spectrometry. Sep Sci Technol 42:3465–3480. https://doi.org/10.1080/01496390701626552
77. Kwiatkowski E, Kwiatkowski M (1980) Unsymmetrical Schiff-base complexes of nickel (II) and palladium (II). Inorg Chim Acta 42:197–202
78. Muraviev D (1998) Solvent Extr Ion Exch 16:381–457. https://doi.org/10.1080/07366299808934533
79. Kalal H, Panahi H, Hoveidi H, Taghiof M, Menderjani M (2012) Synthesis and application of Amberlite xad-4 functionalized with alizarin red-s for preconcentration and adsorption of rhodium (III). Iran J Environ Health Sci Eng 9:1–9. https://doi.org/10.1186/1735-2746-9-7
80. Ummathur M, Malini P, Krishnankutty K (2013) Dioxouranium (VI) complexes of some unsaturated β-diketones. Int J Chem TechNOL Res 5:1–5
81. Foo K, Hameed B (2010) Insights into the modeling of adsorption isotherm systems. Chem Eng J 156:2–10. https://doi.org/10.1016/j.cej.2009.09.013
82. Srinivasan T, Rao P, Sood D (1997) Solvent Extr Ion Exch 15:15–31. https://doi.org/10.1080/07366299708934463
83. Sajjadi S, Meknati A, Lima E, Dotto G, Mendoza-Castillo D, Anastopoulos I, Alakhras F, Unuabonah E, Singh P, Hosseini-Bandegharaei A (2019) A novel route for preparation of chemically activated carbon from pistachio wood for highly efficient Pb(II) sorption. J Environ Manage 236:34–44
84. Lima E, Hosseini-Bandegharaei A, Moreno-Piraján J, Anastopoulos I (2019) J Mol Liq 273:425
85. Elsalamouny A, Desouky O, Mohamed S, Galhoum A, Guibal E (2017) Evaluation of adsorption behavior for U(VI) and Nd(III) ions onto fumarated polystyrene microspheres. J Radioanal Nucl Chem 314:429–437. https://doi.org/10.1007/s10967-017-5389-5
86. Khawassek Y, Masoud A, Taha M, Hussein A (2018) Kinetics and thermodynamics of uranium ion adsorption from waste solution using Amberjet 1200 H as cation exchanger. J Radioanal Nucl Chem 315:493–502. https://doi.org/10.1007/s10967-017-5692-1
87. Orabi A, Atrees M, Salem H (2018) Selective preconcentration of uranium on chitosan Steroyl thiourea prior to its spectrophotometric determination. Sep Sci Technol 53(14):2267–2283. https://doi.org/10.1080/01496395.2018.1445113
88. Cheira M (2015) Synthesis of pyridylazo resorcinol—functionalized Amberlite XAD-16 and its characteristics for uranium recovery. J Environ Chem Eng 3:642–652. https://doi.org/10.1016/j.jece.2015.02.003
89. Afifi S, Mustafa M, El Sheikh E, Gado M (2012) Extraction and determination of thorium and its application on geologic samples using trioctyl phosphine oxide. Arab J Nuclear Sci Appl 45(3):1–16
90. Fouad H, Abu Elenein S, Elrakaiby R, Abdulmoteleb S (2015) A developed spectrophotometric method for thorium determination using alizarin red S dye in different types of its bearing rocks. Int J Sci Res 4:1611–1615
91. Bale M, Sawant A (2011) Solvent extraction and spectrophotometric determination of uranium (VI) with pyridine- 2-carboxaldehyde 2-hydroxybenzoylhydrazone. J Radioanal Nucl Chem 247:531–534. https://doi.org/10.1023/A:1010626409358